Advances in handwriting and drawing:
a multidisplinary approach

Edited by :

Claudie Faure
Paul Keuss
Guy Lorette
Annie Vinter

EUROPIA
Paris - France

A model for the generation of virtual targets in trajectory formation

Pietro Morasso[1], **Vittorio Sanguineti**[1], **Toshio Tsuji**[2]
[1] *DIST, University of Genova (Italy)* – [2] *Faculty of Engineering, Hiroshima University (Japan)*

ABSTRACT: In the framework of kinematic-oriented models of trajectory formation, we propose a model (ξ-model) that consists of a non-linear dynamical system capable of generating, as motor primitives, a family of curvilinear trajectories. The model links shape and speed by means of a common, scalar time base generator that drives the integration of a translational and an angular error.

KEY WORDS: curvilinear trajectories, dynamical models, terminal attractors

1. Introduction

It is known from experiments on reaching that there must be an internal representation of intermediate positions of the target (*current* or *virtual* targets) in addition to the final one. This means that the central nervous system must be able, as a response to perceived or internally generated target stimuli (discrete input representation), to derive *virtual* trajectories (continuous *hidden* representation) that ultimately determine coordinated muscle contractions (detectable output representation).

This paper proposes a biologically plausible dynamic mechanism of virtual trajectory generation that is essentially based on the non-linear integration of suitable *motor errors*, defined from a measurement of the discrepancy between the final target configuration and the current configuration of the end effector.

With the term *configuration* we imply a positional component as well as a component of orientation; in the case of planar trajectories, for example, the former component can be represented by a pair of Cartesian coordinates and the latter one by the orientation of the velocity vector.

In the paper we focus our attention on *primitive* movements, i.e. patterns

determined by a single target specification. In the discussion, we briefly face the problem of complex trajectories, generated by a sequence of target specifications.

Let us designate with $\mathbf{r}_f$ and $\mathbf{r}(t)$ the final and the current position of the target, respectively, and with $\mathbf{r}_{ef}(t)$ the current position of the end effector. In the view of the brain as a non-linear, adaptive dynamical system, a natural approach to trajectory formation is via a pair of weakly coupled non-linear dynamical systems: one which allows $\mathbf{r}$ to relax towards $\mathbf{r}_f$ and the other which *pushes* $\mathbf{r}_{ef}$ towards $\mathbf{r}$. In other papers (MORASSO and SANGUINETI, 92, 93, 94), we particularly address the latter system, whereas in this paper we analyze the former one (ξ-model), further developing previous studies (MORASSO et al., 93).

This approach to trajectory formation is more coherent with *dynamic* models, like VITE (Vector Integration To Endpoint) (BULLOCK and GROSSBERG, 88, 89), than with *static* mechanisms, like the minimum-jerk model (FLASH and HOGAN, 85) or the power-law model (VIVIANI and TERZUOLO, 82).

In general, although the ξ-model can be classified as a kinematic-oriented one – see (PLAMONDON et al., 93) – because it is independent of the actual joint and muscle patterns, it is not completely unrelated from the dynamic processes which underly joint and muscle control and indeed it shares with them the same type of non-linear dynamics.

2. Modeling the speed profile

Stroke generation can be considered in general as the outcome of a dynamical system that smoothly shifts a virtual target $\mathbf{r} = \mathbf{r}(t)$ from an initial position $\mathbf{r}_0$ to a final position $\mathbf{r}_f$.

Let us consider the following parametric model for a generic straight line trajectory:

$$\mathbf{r}(t) = \mathbf{r}_0 + (\mathbf{r}_T - \mathbf{r}_0)\,\xi(t) \tag{1}$$

where the parameter ξ goes from 0 to 1 while time, t, varies from 0 to t_f (t_f is the movement duration). The time profile of the trajectory is completely determined by that of $\xi = \xi(t)$.

Several models were proposed for the velocity profile $\dot{\xi}(t)$ (see PLAMONDON et al. (93) for a comparison); for instance, the application of the *minimum jerk* (FLASH and HOGAN, 85) cost index yields the following expression for $\xi(t)$:

$$\xi(t) = 6\tau^5 - 15\tau^4 + 10\tau^3 \tag{2}$$

where $\tau = t/t_f$, and corresponds to the following speed profile:

$$\dot{\xi}(t) = \frac{30}{t_f}(\tau^4 - 2\tau^3 + \tau^2) \tag{3}$$

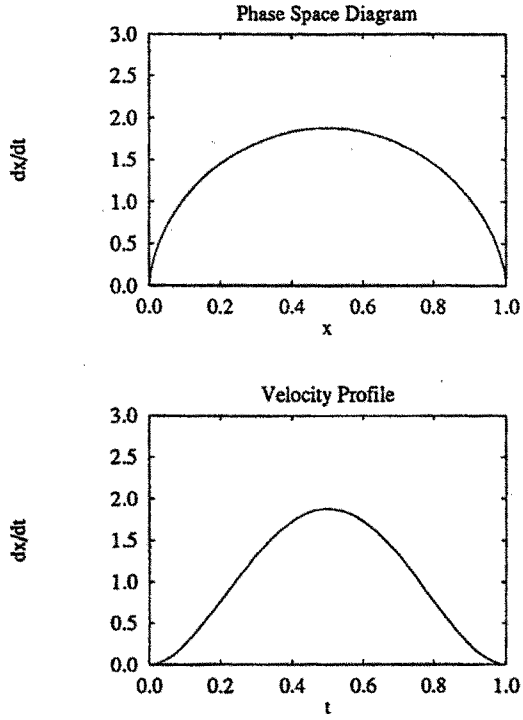

Figure 1. *Phase space diagram (top) and Speed profile (bottom) corresponding to a minimum jerk trajectory*

that is also displayed in Fig. 1 (bottom). However, the main problem with the minimum jerk model, as well as with other kinematic-oriented models, is one of physical implementation, i.e., it is difficult to conceive a biologically plausible mechanism which is able to generate minimum jerk trajectories.

Other kinematic models are focused mainly on the problem of fitting the shape of the speed profile and so are even further from the biological domain. An interesting attempt has been made by (PLAMONDON, 91, 92) in terms of a stochastic approach which applies the central limit theorem to a population of controllers working in cascade fashion. As an alternative, we adopt a deterministic approach and attempt to model the population dynamics with a small set of nonlinear dynamic equations. In particular, we propose that the bell-shaped speed profile is determined by a non-linear dynamical system of

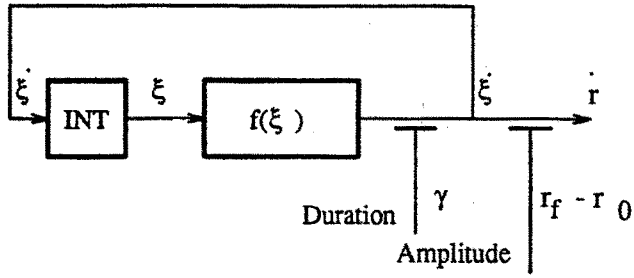

Figure 2. *Block diagram of the dynamical model for trajectory generation*

the type:

$$\dot{\xi} = \gamma f(\xi) \tag{4}$$

where the $f(\xi)$ is implicitly defined by the phase space diagram corresponding to the minimum jerk condition, displayed in Fig. 1 (top), and γ is a gain factor.

One basic requirement on the output of the dynamical system described by Eq. 4 is that ξ should go from 0 to 1 in a *finite time* t_f, whereas $\dot{\xi}$ should tend to zero for $t \to 0$ and $t \to t_f$. In general, t_f is given by

$$t_f = \frac{1}{\gamma} \int_0^1 \frac{d\xi}{f(\xi)} = \frac{K}{\gamma} \tag{5}$$

where K is the area under the inverse of the curve in the phase space (Fig. 1, top), i.e. it is a constant of the dynamical system, so that we can write $\gamma = K/t_f$; therefore, duration is inversely proportional to the gain factor γ. A sufficient condition for attaining a finite value is that $f(\xi)$ is infinitesimal of order n, $n < 1$, for both $\xi \to 0$ and $\xi \to 1$.

The above formulation of the problem of stroke generation may be represented by the block diagram of Fig. 2. Trajectory duration and amplitude are specified by acting on the gains of, respectively, the feedback and the output connections; in particular, as regards the first one, gain is inversely proportional to duration. This representation displays a distinctive feature of the dynamical approach, i.e. the fact that time is not required as a control parameter.

A class of functions $f(\xi)$ that naturally fits the condition of Eq. 5 and has found many applications to non-linear problems in biology and ecology, is a variant of the *logistic growth* model (MURRAY, 89), which is described by:

$$\dot{\xi} = \gamma[\xi(1-\xi)]^e \tag{6}$$

with $e \in (0,1)$. In this case, it can be shown that movement duration t_f is given by:

$$t_f = \frac{1}{\gamma} \frac{\Gamma^2(1-e)}{\Gamma(2-2e)} \tag{7}$$

Under these conditions, the equilibrium configurations of the dynamical system do not satisfy the Lipschitz condition because

$$\left|\frac{df}{d\xi}\right| \to \infty \tag{8}$$

This means that $\xi = 1$ behaves as a *terminal attractor* and $\xi = 0$, which is unstable, is a *terminal repeller* (BARHEN et al., 89). Figure 3 displays the phase space diagrams and the velocity profiles corresponding to different values of e, for $t_f = 1$ s.

The peak speed is reached for $\xi = 0.5$ and is proportional to the parameter γ:

$$\dot{\xi}_{max} = \gamma \frac{1}{2^{2e}} \tag{9}$$

As regards the exponent e, it can be shown that the condition $e \geq 2/3$ is required so that the 3^{rd} time derivative of $\xi(t)$ (*jerk*) exists at $t = 0$ and $t = t_f$. In the simulations presented in next sections we will use $e = 2/3$ because a preliminary comparison with experimental movements showed that it better fits the data than, say, a value of $1/3$. A systematic analysis will be carried out in the future.

The γ parameter has three functions: (i) its transition from 0 to a finite value triggers the time base generator, (ii) its modulation controls movement duration, and (iii) its transition back to 0 can be used to reset the generator and make it excitable for subsequent activation cycles.

In terms of neural network architectures, the block diagram of Fig. 2 may be implemented as a *sequential* neural network, thus reminding the approach proposed by (MASSONE and BIZZI, 89). What is different in the present approach is that different strokes are supposed to be obtained from a common *pattern generator*, possibly made of a kind of sequential neural network. Therefore, different strokes are not represented as different temporal patterns, but are indeed coded in terms of target and timing informations (start time, duration), that are used to modulate the common pattern generator.

Complex tasks, involving multiple targets to be reached with different time constraints or a chain of strokes, may require more pattern generators that work concurrently.

The idea of a parameterized pattern generator also occurs in the work of (HOUK et al., 90), who hypothesizes that the function of the cerebellum is to modulate a set of adjustable pattern generators.

4. Non-linear integration of errors

The dynamical system for trajectory generation described by Eq. 4 and Eq. 1

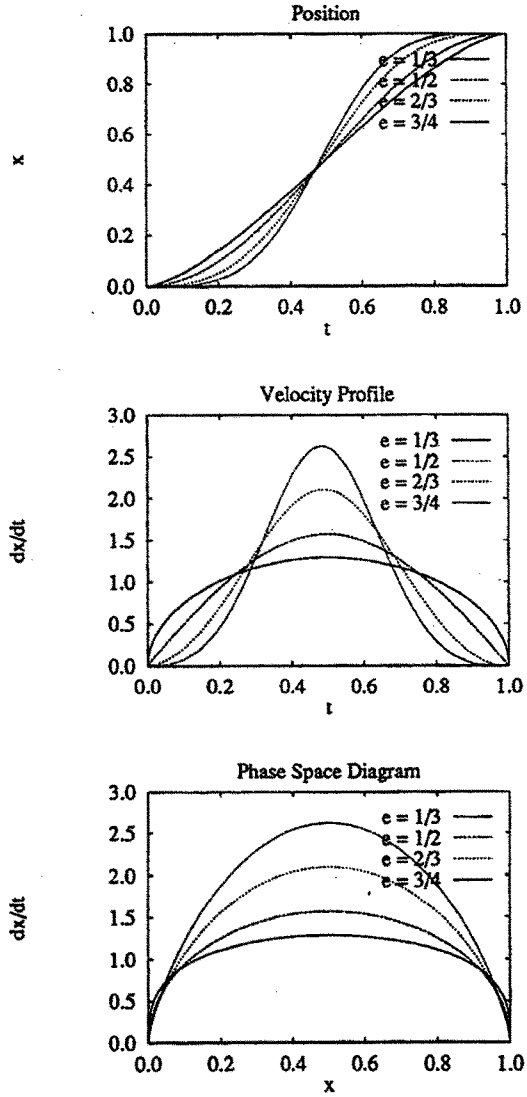

Figure 3. *Output of the target generation mechanism: $\xi = \xi(t)$ (top), $\dot{\xi} = \dot{\xi}(t)$ (middle), and phase-space plot (bottom) for several values of the exponent (1/3, 1/2, 2/3, 3/4)*

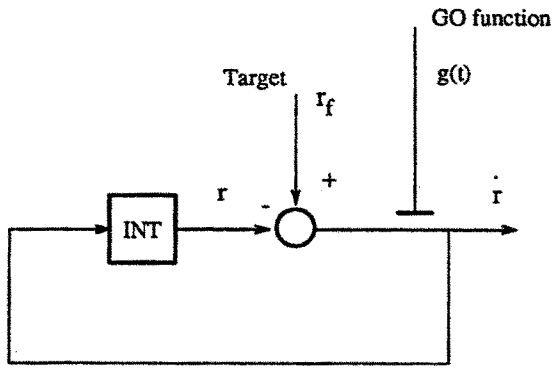

Figure 4. *The VITE model*

may also be expressed in terms of the weighted integration of an error signal $\Delta \mathbf{r} = \mathbf{r}_f - \mathbf{r}$:

$$\dot{\mathbf{r}}(t) = \frac{f(\xi(t))}{1 - \xi(t)} \Delta \mathbf{r} \tag{10}$$

In this form, the model equals to *VITE* (Vector Integration To Endpoint) (BULLOCK and GROSSBERG, 88, 89) and the term

$$g(t) = \frac{f(\xi(t))}{1 - \xi(t)} \tag{11}$$

is what they call *Go-function*: a scalar, increasing function of time that controls the initiation of the movement and the speed profile of the planned trajectory (see Fig. 4). By controlling its shape, it is possible to obtain straight trajectories with any kind of speed profiles; this is a powerful but a too un-constrained mechanism because it leaves ∞ degrees of freedom in the choice of the control signal.

As a matter of fact, deviations of the shape of the speed profile from the purely symmetric case observed in a great variety of experimental situations are remarkably small and we think that it is more economic to model them as a side effect of an intrinsically (quasi)symmetric mechanism, characterized by a small number of parameters (possibly just one), than as the direct consequence of a tunable, general purpose generation system.

The framework of dynamical models allows to specify the constraints on the *Go – function* in order to get a symmetric, bell-shaped speed profile; in particular, it is described by Eq. 11 and is characterized by a single parameter (γ) that linearly modulates peak speed.

Our model (shortly called ξ-model because ξ is the normalized variable of the time-base generator) is a development of *VITE* in two directions: (i) reduction of the number of parameters and (ii) integration of translation and

rotation, in such a way that straight trajectories are just a special case of the dynamic behavior.

The ξ-model includes three kinds of highly interacting dynamic components: a time base generator (with a normalized output variable $\xi = \xi(t)$), a translational motion planner and a rotational motion planner.

4.1. *Straight trajectories*

Let us start with straight movements; without any loss of generality, we can choose a coordinate system with one axis, oriented as the line between the initial and target point, call it r. In this case, the desired directions of the trajectory at the initial and target points must be the same as the direction from the initial point to the target point. As a consequence, we do not need any error term about the direction of the trajectories but just a positional error ($\Delta r = r_f - r$) for which we can define a translational error equation of the following type:

$$\frac{dr}{dt} = \frac{\Delta r}{1-\xi}\dot{\xi} \tag{12}$$

The convergence of this equation, in the case of straight trajectories, can be formally demonstrated in an easy way by defining $\tilde{r} = (r - r_0)/(r_f - r_0)$ from which we get:

$$\frac{d\tilde{r}}{dt} = \frac{1-\tilde{r}}{1-\xi}\dot{\xi} \quad \longrightarrow \quad \frac{d\tilde{r}}{d\xi} = \frac{1-\tilde{r}}{1-\xi} \tag{13}$$

Integrating the latter equation we get the general solution $\tilde{r} = \tilde{r}(\xi) = 1 - c + c\xi$ where c is an integration constant which must be equal to 1 in order to satisfy the initial condition $\tilde{r}(\xi = 0) = 0$. Thus $\tilde{r}(\xi) = \xi$ and the proof of convergence for $r = r(t)$ is obtained.

4.2. *Curved trajectories*

In this section we describe a computational model for the generation of curved trajectories that is an extension of that proposed in the previous sections for rectilinear strokes.

The model is not primarily intended to fit biological data:. although inspired by the above described dynamical approach, it is aimed at solving the problem of generating planar point-to-point trajectories, like those occurring in handwriting movements and, more in general, in robotic applications involving complex curved trajectories (SANGUINETI et al., 93), under the constraints of specified starting and arrival directions.

We assume that curved trajectories are planned in terms of a target point $\mathbf{r}_f$ and a target orientation θ_f in relation to an initial status ($\mathbf{r}_0$, θ_0). For rep-

resenting these trajectories, it is convenient to consider an intrinsic coordinate system where one axis is oriented as the current velocity vector and the other one is perpendicular to it. The dynamics of the model is then described in terms of the linear speed v and the turning speed ω in relation to the goal of simultaneously reaching the target with the desired orientation. For this purpose we can use the same time base generator $\xi = \xi(t)$ and a couple of error measures (a positional error Δr and an orientation error $\Delta\theta$) ending up with a couple of interacting differential equations:

$$v = \frac{\Delta r}{1-\xi}\dot{\xi} \tag{14}$$

$$\omega = \frac{\Delta\theta}{1-\xi}\dot{\xi} \tag{15}$$

The two error terms are defined as follows. The positional term is simply the norm of the difference between the final and the current position:

$$\Delta r = ||\mathbf{r}_f - \mathbf{r}(t)|| \tag{16}$$

The orientation error is more complex and is defined in the following way:

$$\Delta\theta = \Delta\theta_{sym} + 2\sin\theta e^{-\Delta\theta_{sym}^2/2\sigma^2} \tag{17}$$

It is a hierarchical combination (instead of a more common linear combination) of two terms: $\Delta\theta_{sym}$ and $\sin\theta$. In fact, the latter terms becomes more and more relevant (in determining the value of $\Delta\theta$) as the former one decreases. The ***symmetry*** error is defined as $\Delta\theta_{sym} = -(\theta + \theta_f)$ and, as illustrated in Fig. 5, the condition $\Delta\theta_{sym} = 0$ is equivalent to a circular motion.

According to equation (17), it can be seen that while the error term for symmetry is large (i.e. the trajectory is far from circular), the equation (15) is reduced to

$$\frac{d\theta}{dt} = \frac{-(\theta+\theta_f)}{1-\xi}\dot{\xi} \tag{18}$$

which works as a non-linear feedback control law to attain a symmetric configuration. Such a condition is a terminal attractor for the equation which would reach equilibrium at the same time t_f of the time base generator. (This can be shown to hold in a similar way to the demonstration of the previous section.) However, in addition to this dynamic behaviour, the second error term of the angular error expresses a circularity constraint: in any symmetric configuration, there exists a unique circle which goes through both the present and target points and has the present and target direction vectors as tangent vectors.

Fig. 5 illustrates an example of such a circle where O and R represent the center and radius of the circle, respectively. When the trajectory proceeds on a circular arc, the following relation between the angular velocity of the circular arc, ω, and the translational velocity, v, must hold: $\omega = v/R$ (R is the radius

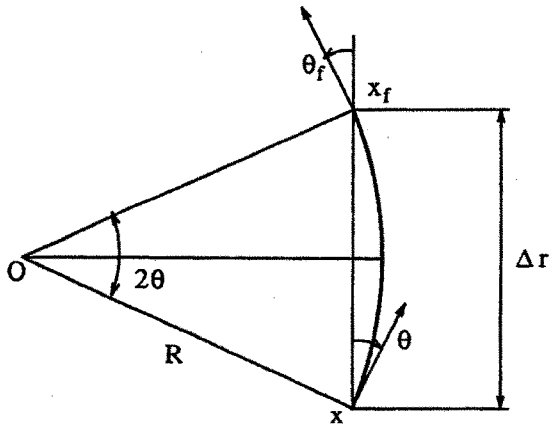

Figure 5. *Geometric constraints in circular trajectories*

of the circle) and since $\Delta r = 2R\sin\theta$ for a circular motion, then we get the differential equation

$$\omega = \frac{2\sin\theta}{1-\xi}\dot{\xi} \tag{19}$$

Thus, if the system starts from a symmetric configuration, the orientation equation (15) is reduced to the previous one and this guarantees the stability of the circular motion. In blending the two terms in the angular error function, the parameter σ measures the speed of relaxation to the symmetric condition and thus the extent of the quasi-circular part of a trajectory.

It is difficult to demonstrate in a formal way the convergence of the overall computational mechanism, i.e. the perfect synchronization between the processes which bring, respectively, $\xi(t_f)$ to 1, $\theta(t_f)$ to θ_f, and Δr to 0. This is so, due to the complex non-linear interactions between the three dynamic processes. However, simulation experiments demonstrated the robustness of the mechanism, suggesting the probable existence of a global Lyapunov function for the overall system.

5. Simulation results

A number of trajectories were simulated by numerically integrating the 3 simultaneous equations (8), (14), and (15) of the ξ-model. For all the figures we used the following values for the parameters: $e = 2/3$ and $\sigma = 0.5$.
In Fig. 6, the initial and target points were fixed, while several initial and target directions satisfying the symmetric configuration condition were used. The figure also shows the profiles of the translational and angular speed. The

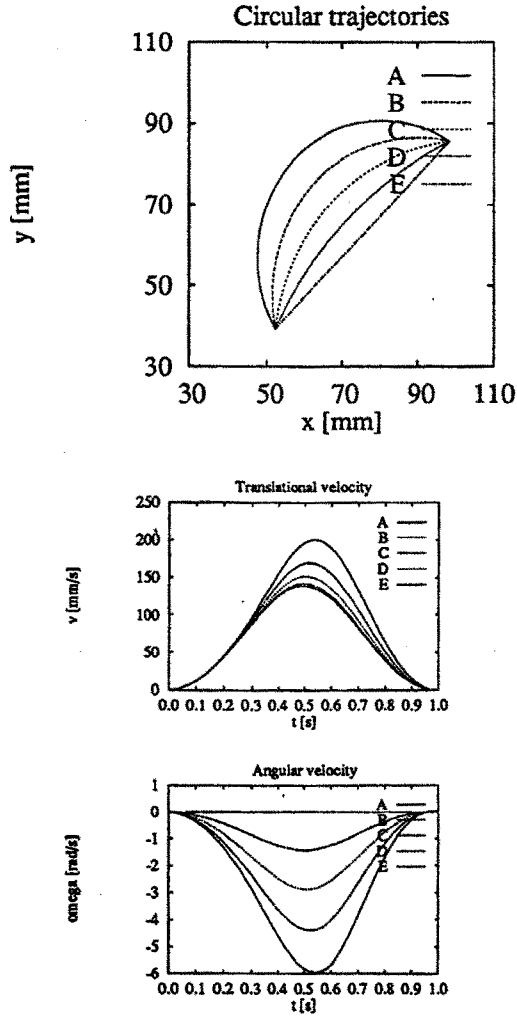

Figure 6. *Simulation of curved movements with symmetric initial conditions. Trajectories (top); translational velocity profiles (middle); angular velocity profiles (bottom)*

former one, in particular, appears to be perfectly symmetric bell-shaped only in the limiting case of straight movements.

Fig. 7 shows experiments with initial symmetry errors of different values (up to 180 degrees). This is a more complex task for the ξ-model. In the initial part of the trajectory, the dominant factor in equation (15) is the reduction of the symmetry error, as it is clearly shown in Fig. 7 (bottom), and this implies a clockwise rotation, until an inflection point is reached. Then, the sense of rotation changes and, in the last part, the trajectory tends to become circular. As shown in Fig. 7 (middle), the speed profile is single peaked if the initial symmetry error is not too big, but can have two peaks in extreme cases.

6. Discussion

The underlying hypothesis in the above described computational model is that circular trajectories are *preferred* by the planning system, as far as they are feasible, whereas more complex, asymmetric situations are solved by reducing a symmetry error.

As displayed from simulations, the model has very good convergence properties and is able to generate very complex trajectories (like the S-shaped ones displayed in Fig. 7, top) in a single step (though the speed profile may have one or two peaks).

What about the biological plausibility of this model? Preliminary observations, performed with a digitizing tablet, have shown that: (i) circular strokes tend to be selected, provided that the initial value of the angular error is not too big, because in this case they would result into a very big radius and therefore a very long path; (ii) an almost linear relationship was found between the initially imposed asymmetry angle and an index of bell-shapedness of the speed profile, measured by the integral square error of the velocity profile with respect to that predicted by the minimum jerk hypothesis for a straight line trajectory. In both cases, if the initial error terms are too big, trajectory is splitted into two or more steps (each denoted by a well marked peak in speed profile).

Apart from biological plausibility, let us express a final comment, regarding the *compactness* of the model. A previous model (MORASSO and MUSSA IVALDI, 82) for handwriting trajectories was based on defining a stroke as a circular arc, which only needs 2 parameters (target distance and radius of curvature), but the representational power is too small because it is necessary to chain at least two strokes even for very simple curved trajectories, which are indeed likely to be derived from a single motor plan.

Regarding minimum jerk models, we have to consider two different versions: the first one (FLASH and HOGAN, 85) is based on a global optimization, whereas in the second one (FLASH et al., 92) minimum jerk is supposed to be applied at the level of single strokes (each corresponding to straight line

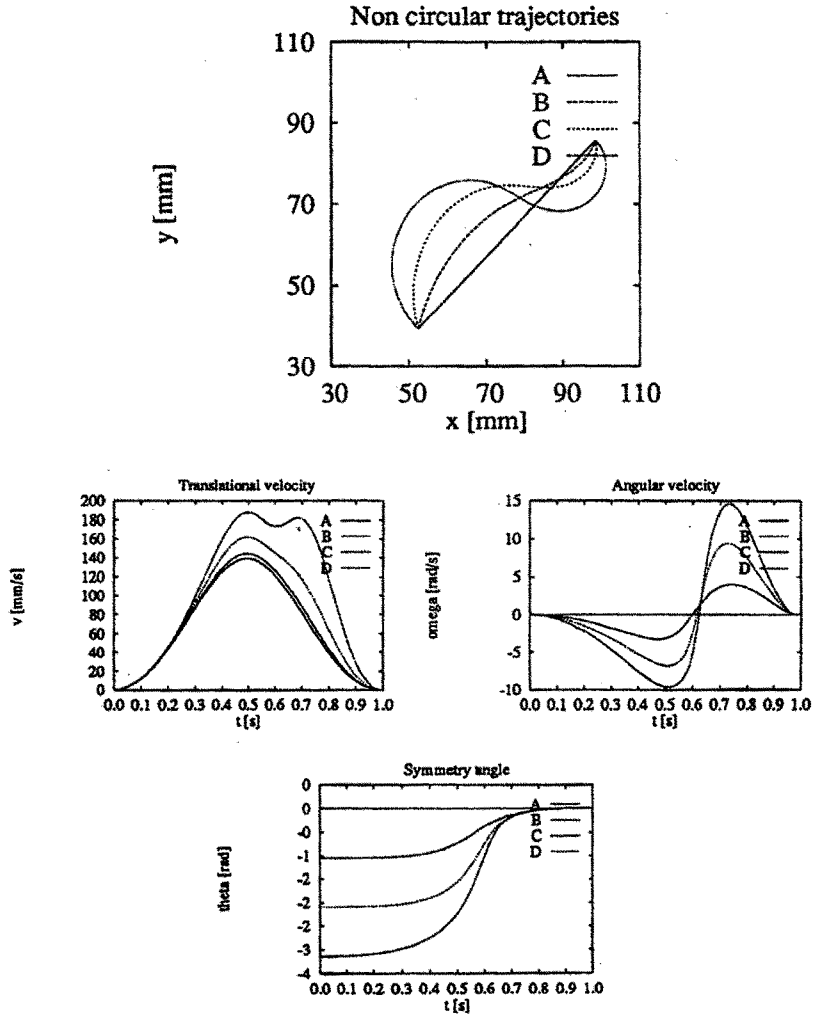

Figure 7. *Simulation of curved movements with non symmetric initial conditions. Trajectories (top); translational and angular velocity profiles (middle); symmetry angle (bottom)*

trajectories).

In the first case, curved trajectories may be specified by one or two *via-points*, thus resulting in 3 to 5 parameters (target distance and the relative coordinates of each via-point). In the second case the number of parameters is the same, but in this case the parameters are target distance and the positions of intermediate targets. However, in both models the number of required parameters depends of the type of trajectory.

Conversely, the present model needs 3 parameters (target distance, initial and final orientations), but is able to represent equally well C-shaped and S-shaped strokes and thus it has a greater representational power; this feature is particularly desirable in a trajectory generation module for robotic manipulators or model-based handwriting recognition systems.

If we consider complex trajectories, a simple composition mechanism, which was already proposed in a previous paper (MORASSO and MUSSA IVALDI, 82), is the linear summation of sequences of strokes appropriately delayed in time, i.e. a coarticulation mechanism. In other words, if we indicate with $\mathbf{r}_i = \mathbf{r}_i(t) = \mathbf{s}_i(t-t_i; \mathbf{p}_i)$ the generic stroke produced by the dynamic mechanism previously described, starting at time t_i and tuned by the parameter vector $\mathbf{p}_i = [\mathbf{r}_f^i, \theta_0^i, \theta_f^i, t_f^i]$, then an arbitrary trajectory can be expressed as follows:

$$\mathbf{r} = \mathbf{r}(t) = \sum_i \mathbf{s}(t - t_i; \mathbf{p}_i) \tag{20}$$

Smooth trajectories require some co-articulation of subsequent strokes and this implies that $t_{i+1} - t_i < t_f^i$, which means that two or more stroke generators must be simultaneously active, although with different activation times, during trajectory formation.

Another mode of operation of this mechanism is the response to a sudden change of the intended target. In this case, it is possible to think that some parameters of a currently active stroke generator are suddenly changed without having to abort it and/or to produce an additional stroke to the new target location.

As regards 3-dimensional trajectories, since some experiments (MORASSO, 83) indicate that trajectories are fundamentally piece-wise planar, it is possible to extend the planar model above simply by adding to each stroke another parameter which specifies the plane of the stroke, e.g. the plane normal vector. In this case, the composition equation (20) is still valid and is capable to produce smooth trajectories with a continuously changing osculating plane.

A future development is to derive a reliable segmentation mechanism which allows to fit real data with equation (20).

References

BARHEN, J., GULATI, S., and ZAK, M., 1989. Neural learning of constrained nonlinear transformations. *IEEE Computer*, *6*, 67–76.

BULLOCK, D., and GROSSBERG, S., 1988. Neural dynamics of planned arm movements: emergent invariants and speed-accuracy properties during trajectory formation. *Psychological Review, 95*, 49–90.

BULLOCK, D., and GROSSBERG, S., 1989. VITE and FLETE: Neural modules for trajectory formation and postural control. In HERSHBERGER, W. (Ed.), *Volitional Action*, pp. 253–297. North-Holland/Elsevier, Amsterdam.

FLASH, T., HENIS, E., INZELBERG, R., and KORCZYN, A., 1992. Timing and sequencing of human arm trajectories: Normal and abnormal motor behaviour. *Human Movement Science, 11*, 83–100.

FLASH, T., and HOGAN, N., 1985. The coordination of arm movements: an experimentally confirmed mathematical model. *Neuroscience, 7*, 1688–1703.

HOUK, J., SINGH, S., FISHER, C., and BARTO, A., 1990. An adaptive sensorimotor network inspired by the anatomy and physiology of the cerebellum. In MILLER, W., SUTTON, R., and WERBOS, P. (Eds.), *Neural Networks for Control*, chap. 14. MIT Press, Cambridge.

MASSONE, L., and BIZZI, E., 1989. A neural network model for limb trajectory formation. *Biological Cybernetics, 61*, 417–425.

MORASSO, P., 1983. Three-dimensional arm trajectories. *Biological Cybernetics, 48*, 187–194.

MORASSO, P., and MUSSA IVALDI, F. A., 1982. Trajectory formation and handwriting: a computational model. *Biological Cybernetics, 45*, 131–142.

MORASSO, P., and SANGUINETI, V., 1992. SOBoS – A Self-Organizing Body Schema. In ALEKSANDER, I., and TAYLOR, J. (Eds.), *Artificial Neural Networks* Amsterdam. North-Holland.

MORASSO, P., and SANGUINETI, V., 1993. Neurocomputing aspects in modelling cursive handwriting. *Acta Psychologica, 82*, 213–235.

MORASSO, P., and SANGUINETI, V., 1994. Self-organizing body-schema for motor planning. *Journal of Motor Behavior.* in press.

MORASSO, P., SANGUINETI, V., and TSUJI, T., 1993. A model for the generation of target signals in trajectory formation. In FAURE, C. (Ed.), *6th International Conference on Handwriting and Drawing* Paris. TELECOM.

MURRAY, J., 1989. *Mathematical Biology.* Springer Verlag, Berlin.

PLAMONDON, R., 1991. On the origin of asymmetric bell-shaped velocity profiles in rapid-aimed movements. In STELMACH, G. E., and REQUIN, J. (Eds.), *Tutorials in Motor Neuroscience*, pp. 283–295. Kluwer Academic Publishers.

PLAMONDON, R., 1992. A theory of rapid movements. In STELMACH, G. E., and REQUIN, J. (Eds.), *Tutorials in Motor behavior II*, pp. 55–69. Elsevier, Amsterdam.

PLAMONDON, R., ALIMI, A. M., YERGEAU, P., and LECLERC, F., 1993. Modelling velocity profiles of rapid movements: a comparative study. *Biological Cybernetics, 69*, 119–128.

SANGUINETI, V., MORASSO, P., and TSUJI, T., 1993. Run-time robot planning. In *International Joint Conference on Neural Networks* Nagoya, Japan.

VIVIANI, P., and TERZUOLO, C., 1982. Trajectory determines movement dynamics. *Neuroscience, 7*, 431–437.

B.P 418.16
75769 Paris cedex 16 - France

Cover design by Stan Vincent
Pastel: Images of writings - Space. Time by Claudie Lenzi

ISBN 2-909285-02-2